Chapter 2

Theoretical background

2.1 Introduction

Before commencing with this study, a number of important topics should be discussed in order to develop a more complete understanding of certain aspects regarding this study. Questions relating to why pulsating B-type stars would be expected to be found in open clusters like the ones chosen for this study, as well as the origin of the pulsating behavior observed in these type of stars, will be addressed in this chapter. These questions are also closely related to other important topics such as, for example, cluster formation, properties of stellar clusters, star formation as a fundamental process and the general evolutionary course of stars. This chapter will serve as theoretical background on most topics addressed in this study.

2.2 Star formation

2.2.1 Giant molecular clouds (GMCs)

The formation of stars is a very important ongoing astrophysical process. Star formation can be seen as one of the main contributing processes in the formation and evolution of galaxies (Kennicutt & Evans, 2012). It is, therefore, important to construct a relevant theory of star formation, which enables the prediction of stellar mass distribution, star formation rate and stellar properties from initial conditions (McKee & Ostriker, 2007). These initial conditions are established in the regions where star formation takes place, which are inside giant molecular clouds (GMCs), existing as an integrated part of the interstellar medium. The interstellar matter consist of gas and dust which are heated and ionised by photons emitted from stars and the mechanical energy released by supernova

explosions of high mass stars (Salaris & Cassisi, 2005). However, star formation takes place in regions of low temperatures, which are found in GMCs, where temperatures are around 20 K (Carroll & Ostlie, 1996). Molecular clouds can be described as self-gravitating, magnetised, turbulent and compressible fluids with gravitationally unstable cores that reside within them (Williams et al., 2000). GMCs range in density between 100 and 300 particles/cm^3, with masses in the order of $10^{5-6} M_\odot$ and extending over $\sim$ 50 parsec (Carroll & Ostlie, 1996, Williams et al., 2000). An upper limit on the mass of GMCs, around $6 \times 10^6 M_\odot$, may be due to tidal effects from the galaxy or the disturbing effect due to massive stars inside the molecular clouds (Williams et al., 2000).

According to Bergin et al. (1997) and Williams et al. (2000), star formation only occurs in the densest regions in these GMCs, called giant molecular cloud cores, from which single stars or multiple systems can be formed. Answers to the important questions on the rate of star formation and the shape of the initial mass function can be obtained by the study of the formation and fragmentation of star-forming clumps inside GMCs. The dense cores can be seen as localised enhancements in the cloud's density profile which are known to be likely regions of low-mass star formation with characteristic sizes of 0.1 parsec (Bergin & Tafalla, 2007). According to Bergin & Tafalla (2007), these dense cores were separated into starless and star-containing classification groups, where the group of star-containing cores were observed to contain young stellar objects. The distinction between the two groups of observed cores, however, depended on the detection threshold, where a detection limit of $0.1 L_\odot$ was possible. The increasing sensitivity, as obtained by the infrared observations done by the Spitzer Space Telescope, led to the discovery of very low luminosity objects, which caused a refinement in the classification of the dense cores. Another type of pre-stellar objects, called dark globules or commonly known as Bok globules, are observed to be dark nebulosities which are separated from any main cloud structure by an external event. They possess lower densities than the dense cores, with sizes and masses up to 1 parsec and $10^3 M_\odot$ respectively (Bergin & Tafalla, 2007).

Although a great deal of uncertainty still encompasses the process of cluster formation and the initial conditions involved in the fragmentation of a star-forming cloud, numerical simulations are being used to simulate these conditions of star formation. In a study done by Klessen et al. (1998), it is shown with the use of numerical simulations that the collapse of a star-forming cloud leads to filamentary structures which fragment into a considerable number of stars. The collapsing molecular cloud undergoes a fragmentation process in which the density increases by many orders of magnitude. During the collapse, the temperature in the cloud remains practically constant as a result of the

increase in density and the radiation of gravitational potential energy from the collapsing cloud, which means that the Jeans mass (see equation. 2.4) should decrease. After instigation of collapse in the molecular cloud, regions of higher density will individually satisfy the Jeans mass criteria and a local collapse will be set off leading to the formation of many smaller structures in the cloud. When the collapse in a smaller structure in the cloud becomes adiabatic, the rise in pressure will decrease the rate of collapse near the core and the central object will reach hydrostatic equilibrium and can be referred to as the protostar (Carroll & Ostlie, 1996).

The Jeans mass used above in describing the process of cloud collapse is the minimum mass necessary to instigate a spontaneous collapse. According to the virial theorem, the condition for collapse is given by $2K < |U|$, where the Jeans mass criteria can be derived by starting with kinetic energy K and the gravitational potential energy, U of a spherical, constant density cloud given by

$$U \sim -\frac{3GM_c{}^2}{5R_c}, \tag{2.1}$$

with the mass and radius of the cloud given by M_c and R_c respectively. The internal kinetic energy K of the cloud, which also appears in the condition for collapse of a molecular cloud is given by

$$K = \frac{3}{2}NkT \tag{2.2}$$

where the total number of particles is given by N. T is the temperature of the cloud and k is the Boltzmann's constant. By substituting the gravitational potential energy and the kinetic energy terms, as defined above, in the condition for the collapse of a molecular cloud and replacing R_c with $R_c = \left(\frac{3M_c}{4\pi\rho_0}\right)^{1/3}$ it follows that

$$\frac{3M_ckT}{\mu m_H} < \frac{3}{5}GM_c{}^2\left(\frac{3}{4\pi\rho_0}\right)^{-1/3} \tag{2.3}$$

The minimum mass necessary to instigate cloud collapse can be solved from equation 2.3 to obtain the Jeans mass relation (equation 2.4)

$$M_J \simeq \left(\frac{5kT}{G\mu m_H}\right)^{3/2}\left(\frac{3}{4\pi\rho_0}\right)^{1/2} \tag{2.4}$$

The Jeans mass can also be expressed in terms of a minimum radius, called the Jeans length $R_J \simeq \left(\frac{15kT}{4\pi G\mu m_H\rho_0}\right)^{1/2}$ (Carroll & Ostlie, 1996).

Because of the fact that GMCs and the pre-stellar cores within them most likely represent a phase before gravitational collapse, valuable information can be obtained on the

topic of star formation, in particular on the distribution of stellar masses, by studying the initial conditions present in these structures which are the starting point for star formation in galaxies (Bergin & Tafalla, 2007). The question on the distribution of stellar masses forming in GMCs and the formation of high mass stars can in turn be addressed when a proper initial mass function is defined.

2.2.2 The Initial mass function (IMF)

General astronomical observations show that stars of different masses form in interstellar molecular clouds. The importance of the stellar mass function in the field of astrophysics lies in the fact that it is used to determine the evolution, surface brightness, chemical enrichment and the baryonic content of galaxies. However, the stellar mass function cannot be observed directly but it can only be determined by transforming the observable luminosity function or surface brightness to the mass function, where the transformation relies on the relationship between mass, age and luminosity (Chabrier, 2003). Because of the dependence of the mass function on the relationship between mass, age and luminosity, the importance of reliable theories of stellar evolution and stellar structure is emphasised, where any uncertainties in these theories will be magnified in determining the IMF (Kroupa, 2002).

Salpeter (1955) defined the initial mass function $\xi(M)$ as shown by equation 2.5, where dN denotes the number of stars in the mass range dM, which were created in the time interval dt, per cubic parsec.

$$dN = \xi(M) d(log_{10} M) \frac{dT}{T_0} \tag{2.5}$$

The mass function as presented by Salpeter (1955) is given by $\xi(M) \approx 0.03(\frac{M}{M_\odot})^{-1.35}$. However, in a more recent study, Kroupa (2002) defined the mass function $\xi(m)$ to be a piece-wise power-law with different values for the slopes of the IMF for each mass interval, shown by

$$\xi(m) = k \begin{cases} (\frac{m}{m_1})^{-\alpha_0} & , m_0 < m \leq m_1 \quad , n = 0 \\ (\frac{m}{m_1})^{-\alpha_1} & , m_1 < m \leq m_2 \quad , n = 1 \\ \left[\prod_{i=2}^{n \geq 2} \left(\frac{m_i}{m_{i-1}}\right)^{-\alpha_{i-1}}\right] \left(\frac{m}{m_n}\right)^{-\alpha_n} & , m_n < m \leq m_{n+1} \quad , n \geq 2 \end{cases} \tag{2.6}$$

where the slope of the power-law is given by α as

$$\begin{array}{lllll} \alpha_0 & = +0.3 \pm 0.7 & , 0.01 & \leq m/M_\odot < 0.08 & , n = 0 \\ \alpha_1 & = +1.3 \pm 0.5 & , 0.08 & \leq m/M_\odot < 0.50 & , n = 1 \\ \alpha_2 & = +2.3 \pm 0.3 & , 0.5 & \leq m/M_\odot < 1 & , n = 2 \\ \alpha_3 & = \begin{smallmatrix} +2.7 \pm 0.3 \\ +2.3 \pm 0.3 \end{smallmatrix} & , 1 & \leq m/M_\odot & , n = 3 \end{array} \tag{2.7}$$

By knowing and comparing the mass distribution of different stellar populations at the time of their formation, the theory of star formation can be enhanced and generalised for a variety of star forming regions.

In the current study, the IMF is of great importance in the understanding of the abundance of high mass star formation in open clusters. The β Cephei stars under study are believed to be stars with masses around $12M_\odot$, which are non-supergiant B-type stars (Stankov & Handler, 2005). Pulsation in β Cephei stars is related to the metallicity which will be discussed later in this chapter. In recent years a number of studies were conducted in order to determine if a relation between the metallicity and the IMF, in star-forming regions, existed. It is expected that the IMF varies with changing star-forming conditions. However, evidence points to a uniform IMF, where it holds for different stellar populations, from old, low metallicity globular clusters to present-day star-forming regions (Kroupa, 2002).

2.3 Stellar evolution

In the field of stellar astrophysics, valuable insight into the important topics of stellar evolution and stellar structure can be obtained from studying stars in different evolutionary phases of their existence. Due to the time scales on which stellar evolution occurs, stars of all possible types need to be observed and classified in order to build up feasible stellar models. In short, the process of stellar evolution can be divided into three main phases, which are

- The process in which stars of different masses form out of gas in the interstellar medium (ISM).
- Tracking the structural changes in evolving stars as a result of the nuclear forces.
- Looking at the final products of stellar evolution after a steady state is reached.

The lower and upper limits in stellar masses are given by $0.08M_\odot$ and $60M_\odot$ respectively (Padmanabhan, 2001). For masses less than $0.08M_\odot$, nuclear reactions cannot

be sustained in the contracting stellar core to form a star by the instigation of nuclear reactions. However in the case where stellar masses exceed $60 - 100 M_{\odot}$, instability will prevent such massive structures from existing for a substantial amount of time. The star Eta Carina is a good example of a high mass unstable star, where it also shows how instability constrain stellar evolution at the top of the HR diagram (Davidson & Humphreys, 1997).

Initially hydrogen fusion is the dominant process taking place in the core regions of stars which are in their first and longest phase of stellar evolution. Hydrogen is fused into helium, where four protons combine to form a helium nucleus, together with the release of approximately 0.03 $m_p c^2$ of energy, which is a fraction of around 0.007 of the original energy, 4 $m_p c^2$. The timescale on which nuclear burning takes place in a star can be defined by $t_{star} = \epsilon M/L$, where ϵ is the fraction of rest-mass energy available for nuclear fusion reactions, M is the stellar mass and L is the luminosity of the star. This timescale will be relevant if the opacity in the star is due to Thompson scattering.
Stars in this steady nuclear burning phase are called zero-aged main-sequence (ZAMS) stars, which will exhaust their hydrogen after a time, $t \gtrsim t_{star}$ (Padmanabhan, 2001).

Although the underlying processes involved in stellar evolution, can be regarded as uncomplicated, the number of possible combinations in a stellar evolutionary cycle relies heavily on the different stellar properties and initial conditions during the star formation process (Padmanabhan, 2001).

2.4 Stellar structure

Stars can be modelled as gravitating gas spheres in hydrostatic equilibrium, which are powered by nuclear fusion reactions and the release of gravitational energy. The topic of hydrostatic equilibrium will be of central importance during the explanation of the mechanism behind the pulsating behaviour of the β Cephei stars. With the brief background in stellar evolution and formation, the topic of stellar structure will occupy a central role in this study. There will be focused on ionisation in stars, opacities in stellar atmospheres, which plays an important role in the pulsation modes in stars, and also on the stellar equations of state, which are used in stellar models.

2.4.1 Hydrostatic equilibrium

Hydrostatic equilibrium is the mechanical equilibrium in a star where the two opposing forces, gravity and the pressure in the star, balance each other. The force of gravity

is directed inwards, towards the centre of the star, while the pressure gradient has the effect of a resultant outward force with the same absolute magnitude as the gravitational force, in order to achieve hydrostatic equilibrium (Kippenhahn & Weigert, 1994). The derivation for the equation, describing the condition for hydrostatic equilibrium, is given in, for example, Kippenhahn & Weigert (1994), where the equation is given in the Lagrangian form by

$$\frac{\partial P}{\partial m} = -\frac{Gm}{4\pi r^4} \tag{2.8}$$

However, stars may not always be confined to the state of hydrostatic equilibrium, they may deviate from this condition by means of expansion and contraction during their lifetime or the display of pulsating behaviour. In order to describe the radial accelerating motion in expanding and contracting stars, where the sum of the pressure and gravitational force is not equal to zero, the acceleration of a mass shell can be described by

$$\frac{dm}{4\pi r^2}\frac{\partial^2 r}{\partial t^2} = f_P + f_g, \tag{2.9}$$

where the term on the left gives the force per unit area on the accelerating mass shell. f_P and f_g denote the forces on the mass shell due to pressure and gravitational forces respectively. By substituting these two forces into Equation 2.9, it yields the equation of motion, which will reduce to the equation of hydrostatic equilibrium if the second derivative of r with respect to time, or in other words the acceleration, is zero (Kippenhahn & Weigert, 1994).

The virial theorem that was mentioned earlier, is of central importance in the understanding of stars due to the fact that it links two stellar energy sources. Some evolutionary phases are also predictable by the use of the virial theorem (Kippenhahn & Weigert, 1994). The two important energy sources linked by the virial theorem are the gravitational energy E_g, and the total internal energy E_i of the star, related by $E_g = -2E_i$ (Kippenhahn & Weigert, 1994). The gravitational and internal energy as defined by Kippenhahn & Weigert (1994), are given by

$$\begin{aligned} E_g &= -\int_0^M \tfrac{Gm}{r}\, dm \\ E_i &= \int_0^M u\, dm \end{aligned} \tag{2.10}$$

where G is the gravitational constant, r is the stellar radius, m is the mass and $u = c_v T$ is the specific heat per unit mass at constant volume.

2.4.2 Chemical composition

The initial chemical composition of stars that form in a molecular cloud will be determined by the local composition of the ISM from which the cloud is composed. One of the most frequently used composition parameters can be quantified in terms of the iron to hydrogen ratio, which is also better known as the metallicity. The metallicity is commonly defined as

$$\left[\frac{Fe}{H}\right] \equiv log_{10}\left(\frac{N_{Fe}}{N_H}\right) - log_{10}\left(\frac{N_{Fe}}{N_H}\right)_{\odot}, \tag{2.11}$$

where $\left[\frac{Fe}{H}\right]$ is the ratio of iron to hydrogen and N_Fe and N_H denote the number of iron and hydrogen atoms per unit volume. From this equation it can be seen that the ratio of Fe to H in a star under study is compared to the same ratio observed in the Sun. Therefore $\left[\frac{Fe}{H}\right] = 0$ when a star has the same element abundances as found in the Sun (Carroll & Ostlie, 1996). Because of the fact that metal enrichment in the ISM is a result of supernova explosions and mass loss from lower mass stars, iron content in stars should also give an indication of stellar age, meaning that younger stars tend to have a higher metal content than older stars, which is referred to as the age-metallicity relation. However, the reliability of age determination by the use of this method is questionable due to the long time scales in which type Ia supernovae appear after star formation and the homogeneity of the ISM enrichment thereafter (Carroll & Ostlie, 1996). According to Salaris & Cassisi (2005), Type II supernovae eject mainly α-elements (O, Ne, Mg, Si, S, Ca and Ti) into the ISM, where Type Ia supernovae are mainly responsible for the iron enrichment. For this reason a smaller α/Fe ratio will be an indication of younger generation stars, while a larger ratio indicates older generation stars.

The importance of the chemical composition lies in the fact that it affects key stellar properties like the transport of radiation and the production of energy by nuclear processes (Kippenhahn & Weigert, 1994). The opacity that will be described in the next section is also greatly affected by the element abundances in the stellar atmospheres, which is also a key property in stellar pulsations.

2.4.3 Opacity

Opacity is defined as the property of a medium which regulates how it absorbs or scatters electromagnetic radiation. This property is dependent on the composition, temperature, density of the medium, and on the wavelength of the electromagnetic radiation passing through the medium (Ridpath, 2012).

Scattering and absorption can be seen as two processes which effectively result in the removal of photons from a beam of parallel light rays that passes through a gas. The removal of photons from the beam of light rays will consequently change the intensity of the beam, where the change in intensity can be given by

$$dI_\lambda = -\kappa_\lambda \rho I_\lambda ds, \tag{2.12}$$

where ds is the distance travelled through the gas, ρ is the density, and κ_λ is the wavelength dependent absorption coefficient or the opacity of the medium. By the integration of equation 2.12, the final intensity of the beam can be found which travelled a distance s through the gas. If the gas is assumed to have a constant density and opacity, the final intensity is given by

$$I_\lambda(s) = I_{\lambda,o} e^{-\kappa_\lambda \rho s}, \tag{2.13}$$

were $I_{\lambda,o}$ denotes the initial intensity of the beam (Rybicki & Lightman, 1979, Carroll & Ostlie, 1996).

The importance of stellar composition is emphasised when the four primary sources of opacity are investigated. These sources are the following:

- **Bound-bound transitions** occur when electrons make transitions between different orbital states through the absorption of photons with appropriate energies. Bound-bound transitions are responsible for the observable spectral lines in stellar spectra, where electrons in excited states can emit photons in the process of returning to lower energy states. If an electron makes a transition from a lower to a higher state, with the absorption of a photon, it results in absorption lines in the continuous spectrum of the source.

- **Bound-free absorption** is the result of energetic photons that ionise atoms by removing electrons from the atoms through a process known as photoionisation. The contrary can also occur where a free electron recombines with an atom associated with the emission of one or more photons.

- **Free-free absorption** explains the process of a free electron-ion unbound pair absorbing or emitting a photon with a resulting increase in the speed of the electron with the absorption of the photon and a decrease in its speed with the emission of a photon. The process of photon emission is also known as "bremsstrahlung". Due to the fact that this process occurs for all wavelengths, it is an important contributor to the total opacity in stellar atmospheres.

- **Electron scattering** takes place when photons are scattered off electrons in a process called Thompson scattering. This process is also wavelength independent but since the cross section for Thompson scattering is very small, this process only contributes significantly to the total opacity at high temperatures where most gas is completely ionised (Böhm-Vitense, 1993, Carroll & Ostlie, 1996).

Due to the difficult nature of opacity calculations, which is due to the great number of atoms and molecules that affect the opacity in stellar atmospheres, opacity tables are used to obtain opacity values for different stellar envelope mixtures and compositions. As a result of the advancement in atomic physics in recent years, the modelling of the opacity in the stellar envelope has improved considerably, which will lead to improvement in stellar models (Iglesias & Rogers, 1991).

2.5 Open galactic clusters

Stars do not form independently, but tend to form in clusters, where the cluster stars are products of the same interstellar cloud where they are gravitationally bound and dynamically related (de La Fuente Marcos, 1998, Nilakshi et al., 2002). The properties of these stellar clusters enable them to be used as laboratories for studying different stellar populations where a typical stellar sample contains stars of the same age, distance, initial composition and where only variation in the mass range occurs (Lata et al., 2011). Young open stellar clusters also provide the opportunity to study ongoing star formation which will shed light on a possible IMF, where the study of older open clusters is important for assessing stellar evolution models and understanding the dissociation of open clusters (Battinelli & Capuzzo-Dolcetta, 1991, Brown, 2001). The study of open clusters does not only contribute to the investigation of star formation and evolution but also to the understanding of galactic structure on a larger scale. Young stellar clusters can also be used to map the rotation curve of the Galaxy by analysing the spiral arm structure (Friel, 1995).

In order to describe the population of galactic open clusters, information on cluster formation and formation rates as well as their destruction is necessary. In a study done by Battinelli & Capuzzo-Dolcetta (1991) on the formation and evolutionary properties of galactic open clusters, it was found that the cluster formation rate in a sample of clusters within 2 kpc from the sun, is 0.45 clusters kpc^{-2} Myr^{-1}. It was also suggested that the average lifetime of clusters be around 10 Myr. However, these short lifetimes could not be explained by referring to destructive processes taking place in the galactic disk, but it was ascribed to young clusters born as unstable systems. In a study done by Friel

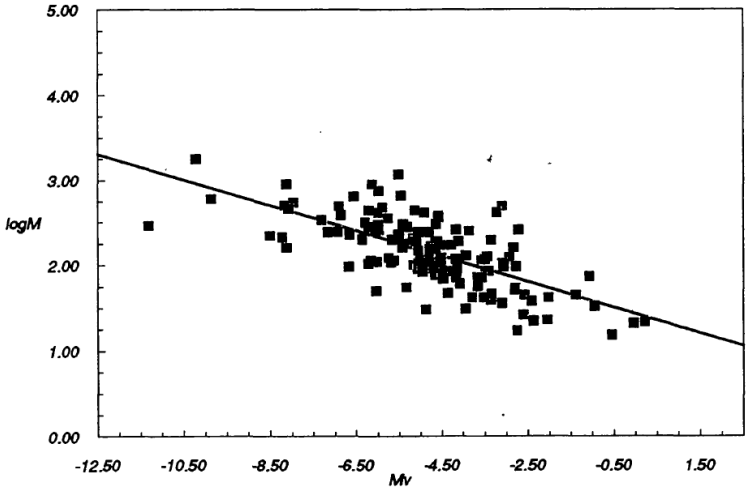

FIGURE 2.1: Mass-luminosity relation of 400 galactic open clusters as given by Battinelli et al. (1994)

(1995), early statistics also showed an under abundance in old open clusters, destroyed by disruptive effects, but after the population was interpreted using the assumption of a uniform destruction rate, it became clear that there existed a substantial population of high aged galactic open clusters.

The understanding of cluster formation is closely related to the initial mass function of open clusters. In a study done by Battinelli et al. (1994) on the photometric properties of open clusters, the masses of 400 open clusters were calculated in order to construct a well defined present-day mass function. Battinelli et al. (1994) presents a photometric assessment of the total mass of a cluster, given by

$$M = \int_0^\infty m\psi(m)dm \simeq \int_{m_{lim}}^\infty m\psi(m)dm = \int_{L_{Vlim}}^\infty m(L_V)\phi(L_V)dL_V, \tag{2.14}$$

where $\psi(m)$ and $\phi(L_V)$ are the respective mass and V-band luminosity functions of the cluster. m_{lim} is the limiting mass which corresponds with the limiting luminosity L_{Vlim}. The present-day mass function for these 400 clusters was then constructed from the calculated cluster masses, where a mass-luminosity relation was also created for these clusters under study. The mass-luminosity relation is shown in Figure 2.1, where the relation is given by $\log M = -0.15M_V + 1.43$. However current observations of clusters can only reveal the present day mass function, where mass loss occurred through the dynamical evolution and stellar evaporation of the clusters. Another contributing factor that can also result in cluster mass loss, is the tidal shock on the cluster by passing through the galactic disk (Kroupa, 2002). Establishment of the mass distribution of galactic open clusters is more challenging than to determine that of globular clusters. The reason for this can be found in the wide range of distances and ages of galactic open clusters, where the conversion from a luminosity function to mass function is age

dependent. Because of the wide age range, the currently observed luminosity distribution should differ from the initial mass distribution which makes it difficult to determine the latter. From this it can be seen that the construction of the initial cluster mass function relies strongly on stellar evolution models, where stellar evolution should be applied in reverse, in order to create a viable initial mass function from a present-day mass function (Elmegreen & Efremov, 1997).

These properties of galactic open clusters and the study of open clusters in general are very important in order to form a better understanding of the conditions in which these specific stars under study exist.

2.5.1 Interstellar extinction and reddening

Because of the fact that the interstellar medium is permeated with gas and dust, starlight is affected by the interstellar matter on its way to the observer on Earth. The losses of propagating stellar radiation by the interaction with the interstellar medium, through absorption and scattering, is collectively referred to as interstellar extinction (Salaris & Cassisi, 2005).

The process of absorption can be described by referring to the intensity of light, I, passing through a medium. The change in the intensity, due to absorption, is given by

$$I_\lambda / I_{\lambda,o} = e^{-\tau_\lambda}, \tag{2.15}$$

where $I_{\lambda,o}$ and I_λ are the observed and initial intensities. If the particle scattering cross section σ_λ, along the line of sight can be assumed constant, the optical depth can be defined as

$$\tau_\lambda = \sigma_\lambda N_d, \tag{2.16}$$

where N_d is the column density, which is defined as the number of scattering particles, along the line of sight, in a cylinder with cross sectional area of 1 cm^2. If equation 2.15 is converted to magnitude, it results in the change in apparent magnitude as a result of extinction given by

$$\begin{aligned} m_\lambda - m_{\lambda,o} &= -2.5 \log_{10} e^{-\tau_\lambda} \\ &= 2.5 \tau_\lambda \log e \\ &= 1.086 \tau_\lambda \end{aligned} \tag{2.17}$$

Interstellar extinction can now be defined as the change in magnitude due to extinction given by $a_\lambda = 1.086\tau_\lambda$ (Carroll & Ostlie, 1996). From this it can be seen that the

apparent magnitude of an object needs to be corrected for extinction. This can be done by modifying the distance modulus, $m_\lambda - M_\lambda$, by adding the number of magnitudes due to absorption and extinction as given by

$$m_\lambda - M_\lambda = 5 \log_{10} d - 5 + a_\lambda, \tag{2.18}$$

where m_λ and M_λ represent the apparent magnitude and the absolute magnitude respectively and d is the distance in parsec.

Due to the fact that the extinction is wavelength dependent, shorter wavelengths tend to be absorbed and scattered more than longer wavelengths. This phenomenon gives rise to the reddening effect of starlight. As a result of interstellar reddening, the colour of stars, expressed as $(B - V)$, is not the same as the true colour because of interstellar extinction. Consequently interstellar reddening is defined as

$$E(B - V) = (B - V) - (B - V)_0, \tag{2.19}$$

where the subscript 0 refers to the true colour of the star. Equation 2.19 can be rewritten as

$$E(B - V) = (B - B_0) - (V - V_0), \tag{2.20}$$

where $(B - B_0)$ and $(V - V_0)$ are the extinction in the B and V band, denoted by A_b and A_v respectively.

According to Rieke & Lebofsky (1985), $\frac{A_b}{A_v} = 1.324$, so that Equation 2.20 can be written as

$$E(B - V) = 1.324 A_v - A_v \tag{2.21}$$

From this it is possible to obtain the reddening value $E(B - V)$ from the WEBDA database (`http://www.univie.ac.at/webda/navigation.html`), in order to determine the visual extinction for the B and V band for both clusters in this study. The extinction calculations for both clusters, by using information from the WEBDA database is shown in Appendix A.

With the effects of extinction and reddening in mind, it is easy to understand the corrections that need to be applied to Padova stellar evolution models, before adding these models to a colour magnitude diagram of the two clusters under study. Figure 2.2 shows the stepwise correction to a stellar evolution track in order to add the track to a colour magnitude diagram from the two clusters presented in this study. The uncorrected evolutionary track is shown in red, where distance and reddening needs to be corrected for. The green evolutionary track resulted from applying the distance correction to the uncorrected red track. This was done by adding the visual extinction magnitude to the

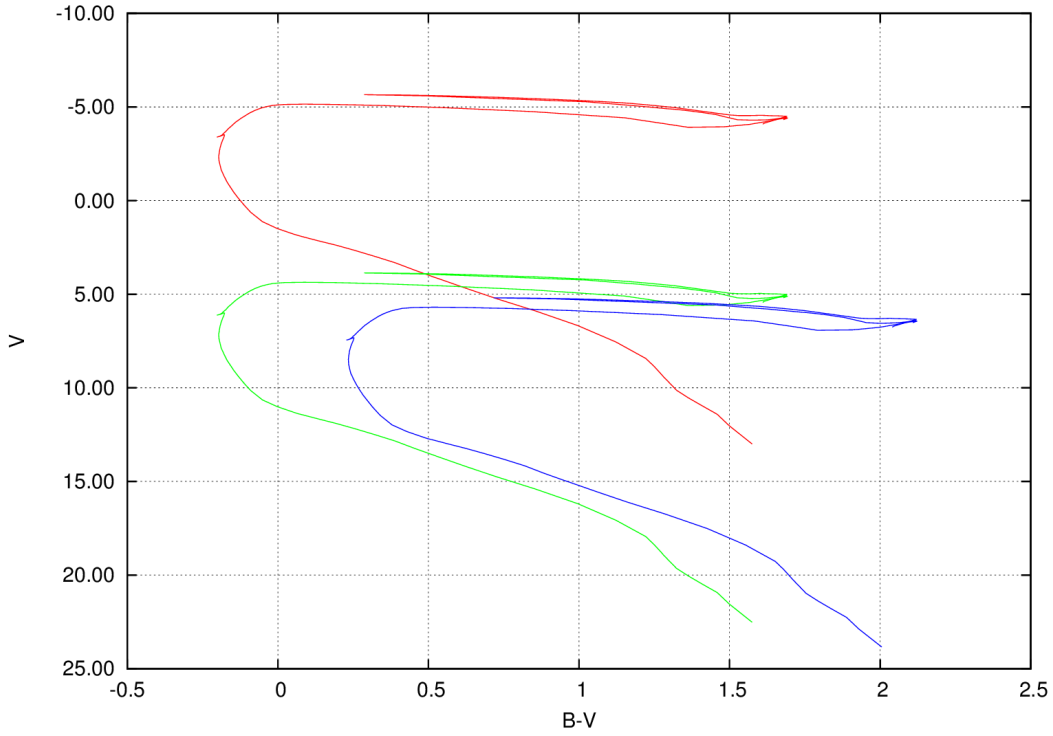

FIGURE 2.2: The simultaneous correction of the distance and reddening to the Padova stellar evolutionary track shows a diagonal movement to the lower right side of the diagram. The uncorrected red evolutionary track is corrected for distance, resulting in the green track, where the green track is corrected for reddening, which gives the blue track.

V band data of the model, where it is clear that this correction causes the evolutionary track to move downwards on the diagram. The final track in blue shows the reddening correction to the evolutionary model, which indicates a downward movement to the right hand side of the diagram. This reddening correction can also be seen as a correction in (B-V) which is also synonymous to the colour of a source.

2.6 Classification of variable sources

The general classification of variable and periodic sources relies strongly on previous observational data and classification schemes of variable stars. The classification of the sources found from this study will be explained in more detail in Chapter 4. However, in what follows, a brief introduction and description of two important B-type stars will be given, where the search for β Cephei stars was also part of the main motivation behind this study.

2.6.1 Classification and properties of B-type pulsating stars

2.6.1.1 β Cephei stars

For more than 100 years, β Cephei stars have been observed and studied. Variability of this type of star was discovered in 1902 by Edwin Brant Frost, who carried out a series of spectroscopic observations, from which the radial velocity variation of the star β Cephei was measured. Figure 2.3 illustrates the provisional radial velocity curve for the star β Cephei as presented by Frost (1906). At first Frost (1906) concluded that β Cephei was a spectroscopic binary with an estimated period of $4^h34^m11^s$. However, later work indicated that the star β Cephei is in fact a pulsating star. The star β Cephei later became known as the prototype star to the class of β Cephei variable stars (Lesh & Aizenman, 1978).

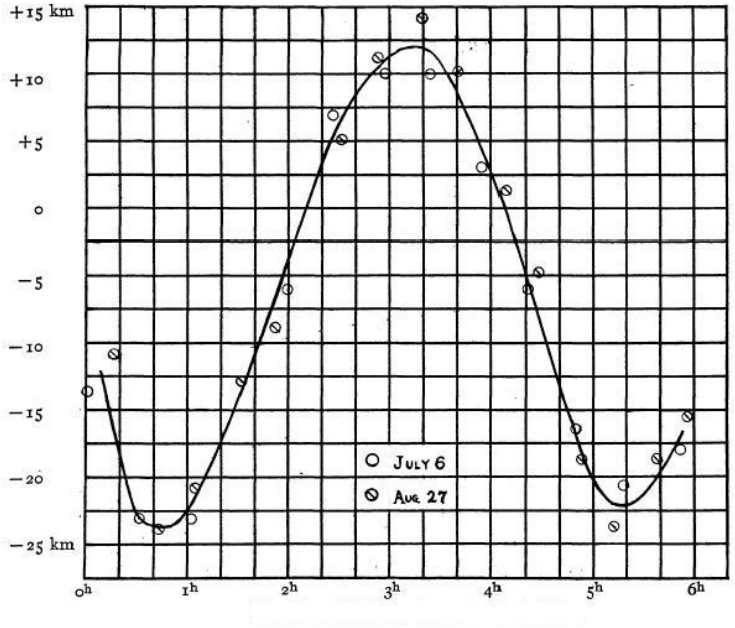

FIGURE 2.3: Provisional radial velocity curve presented by Frost (1906)

β Cephei stars, as they are commonly known today, are early B-type stars which exhibit short-period brightness variations, radial velocity variations and a strong line profile variation, where the latter property also simplifies the detection of small amplitude radial velocity variations. Their amplitudes in light variation increases towards shorter wavelengths which is an indication of temperature variations of the star (Lesh & Aizenman, 1978, Sterken & Jerzykiewicz, 1992). One of the most eluding properties of these variable stars is the mechanism behind their pulsating behaviour, which will be addressed later on. These long term pulsations must be sustained by a mechanism of vibrational instability, where pulsation periods between 1.60 and 7.66 hours have been recorded (Sterken & Jerzykiewicz, 1992, Stankov & Handler, 2005).

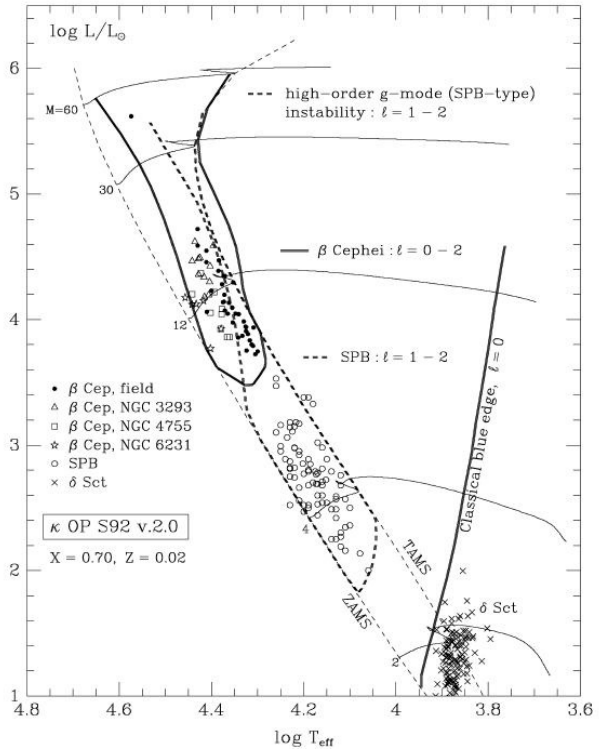

FIGURE 2.4: Hertzsprung-Russell Diagram reproduced from Pamyatnykh (1999), showing instability regions in the upper main sequence

As a definition of the class of β Cephei stars, Stankov & Handler (2005) proposed that β Cephei stars are massive non-supergiant variable stars, with spectral type O or B whose light, radial velocity and/or line profile variations are caused by low-order pressure and gravity mode pulsations. These pulsations then result in radial velocities which are usually observed to be less than 50 km sec^{-1}. In the class of β Cephei variables, the radial velocity curve leads the light curve by 90 degrees, which is different from what is observed in the classical Cepheid variables and RR Lyrae stars. This fact causes the maximum brightness and temperature to correspond to minimum radius of the star, while minimum brightness and temperature coincides with maximum radius (Lesh & Aizenman, 1978).

The class of β Cephei stars can be indicated by a well-distinguished region or ″instability strip ‶on the Hertzsprung-Russell Diagram (see Figure 2.4), with spectral type ranging from B0.5-B2 and luminosity classes of (II-III)-IV (Lesh & Aizenman, 1973). This region is located in Figure 2.4 above the zero age main sequence for early B-type stars (Lesh & Aizenman, 1978).

Pulsation in β Cephei stars is believed to be a result of the opacity driven κ-mechanism, where Moskalik & Dziembowski (1992) were first to introduce this concept to the problem

of β Cephei pulsations. In order to study pulsations of this type, it is necessary to first take a look at the underlying opacity driving mechanism.

In a study done by Baker & Kippenhahn (1962) on pulsation models of δ Cephei stars, it was explained that an increase in the absorption coefficient or opacity of certain layers of the star during maximum compression will lead to the confinement of radiative energy in the specific layer or region, which will result in a subsequent expansion. This mechanism which is dependent on the pressure and temperature dependence of the absorption coefficient κ, will then be the driving mechanism behind the pulsation called the κ-mechanism, which was first introduced by Baker & Kippenhahn (1962) (Baker & Kippenhahn, 1962, King & Cox, 1968).

The opacity κ of gas inside a star decreases as temperature increases where the Rosseland mean κ depends on the density ρ and temperature T as $\bar{\kappa}_R \propto \rho T^{-3.5}$ (Böhm-Vitense, 1992). There are, however, some regions in which this relation can be reversed. The opacity bump caused by helium ionisation was first proposed by Stellingwerf (1978) as the driving mechanism behind β Cephei pulsations. This small bump in opacity was discovered to be at a temperature close to 1.5×10^5K, and produces a trend towards increased opacity with contraction of the pulsating star, which in turn has a destabilising effect on the star (Stellingwerf, 1979). This mechanism, which is similar to the κ-mechanism, effects the pulsation in regions where the main destabilisation is due to ionisation of hydrogen and helium. However, it was found that this feature was not strong enough to cause instability of the radial or non-radial modes (Moskalik & Dziembowski, 1992). Simon (1982) proposed an increase in the metal opacities by a factor of 2-3 in the temperature range between 10^5 K and $2 \times 10^6 K$, which would result in the desired opacity bump. In a study done by Pigulski & Kołaczkowski (2002) on Early-type variables in the Magellanic clouds, three β Cephei stars were found, where it was indicated that these β Cephei stars have metallicities higher than the average metallicity found in the Large Magellanic Cloud. Pigulski & Kołaczkowski (2002) suggested that this is a strong observational confirmation that the driving mechanism is dependent on the metallicity in these pulsating stars, where only a few were found in the Magellanic clouds because of their lower metallicity.

β Cephei pulsators can be seen as a very useful probe of distances and composition of stellar systems (Moskalik & Dziembowski, 1992). Another important relation was found by Balona et al. (1997), where the excited frequencies of pulsating stars of a given age are correlated with the mass. The slope of the frequency-mass diagram was found to be very responsive to age, where this relation can also be used to determine ages of stellar clusters more accurately than with the use of isochrone fitting (Balona et al., 1997).

2.6.1.2 Slowly pulsating B-type stars

This class of B-type variable stars is main sequence B2-B9 stars which show both light and line profile variability and which pulsate in high radial order g-modes. Pulsation periods may range from 0.4 - 5 days with amplitudes smaller than 0.1 magnitudes (The International Variable Star Index, 2012). On the HR diagram, the SPB region is found below the β Cephei instability strip as indicated on Figure 2.4.

Both β Cephei and slowly pulsating B stars (SPB) stars are destabilised by the κ mechanism operating on the the metal opacity bump as described in the previous section, where the unstable modes are in close agreement with the observed pulsation periods of 0.5 - 4.1 days Moskalik (1995). Although SPB stars, with periods longer than 0.5 days, have been found in the LMC, it creates a greater challenge observing these stars outside the Galaxy because of lower luminosity and longer period variability than the β Cephei stars (Kołaczkowski et al., 2004). According to Pigulski & Kołaczkowski (2002) and references therein, the LMC and SMC have lower than galactic metallicities. This fact can be used as a tool to study the instability mechanism in these B-type stars where it is also stated by Moskalik (1995) that the β Cephei pulsations disappears at metallicities of $Z < 0.012$, while for SPB stars, their pulsations will vanish at a lower metallicity of $Z < 0.006$. By knowing this sensitivity of the instability of both these B-type stars, it can be used in determining the lower limit of metal abundances in stellar systems.